Subphase pH Effect on Surface Micelle of Polystyrene-*b*-poly(2-vinylpyridine) Diblock Copolymers at the Air−Water Interface

Bonghoon Chung,† Myunghoon Choi,† Moonhor Ree,† Jin Chul Jung,‡ Wang Cheol Zin,‡ and Taihyun Chang*,†

Department of Chemistry, Department of Materials Sciences and Engineering, and Polymer Research Institute, Pohang University of Science and Technology, Pohang 790-784, Korea

Received September 21, 2005; Revised Manuscript Received November 10, 2005

ABSTRACT: The subphase pH effect on the surface micelles of polystyrene-*b*-poly(2-vinylpyridine) (PS-*b*-P2VP) diblock copolymers was investigated by the $\pi-A$ isotherm and the morphology of the Langmuir−Blodgett (LB) film. Ionization of P2VP block significantly affects the $\pi-A$ isotherm of the surface micelles at the air−water interface. At high pH, where the degree of ionization is low, the $\pi-A$ isotherm shows a more expanded form and high transition surface pressure reflecting the strong tendency of P2VP blocks spreading on the subphase surface. As the subphase pH is lowered, the transition surface pressure decreases while the transition region is more extended, indicating the facile equilibrium between the flotation and submergence of the P2VP blocks upon surface pressure change. At pH 1.8 at which the 2VP units are completely ionized, the ionized P2VP blocks submerge into the subphase even at low surface pressure, and the transition behavior is not observed. The $\pi-A$ isotherm behavior can be understood considering the balance of the solubility and the electrostatic repulsion of the ionized P2VP chains. Atomic force microscopy images of the LB films of the PS-*b*-P2VP surface micelles show isolated circular micelles at high pH. As the subphase pH decreases, the intermicellar distance becomes shorter and the micelles eventually contact each other to form a laced network of circular micelles. The association behavior of surface micelles and the $\pi-A$ isotherms at low pH are strongly dependent on the ionic strength of the subphase. The linear association of the surface micelles at low pH appears to result from the balance of the hydrophobic attraction among the floated PS cores and the electrostatic repulsion among the submerged P2VP chains. On the other hand, the average aggregation number of each surface micelle is independent of subphase pH, which indicates that the aggregation of the block copolymers to form surface micelles is likely to take place before the P2VP blocks are ionized.

Introduction

Many amphiphilic block copolymers can self-assemble at the air−water interface into various microphase-separated structures, which are called surface micelles.[1−8] The hydrophobic blocks aggregate to form isolated structures of different shapes mainly depending on the block copolymer composition, which are stabilized by surface-active hydrophilic blocks spread on the water surface. Following the first report on the surface micelle morphology by Zhu et al., many works have been reported on the surface micelle behavior of various amphiphilic block copolymers at the air−water interface: polystyrene-*b*-poly(vinylpyridine) (PS-*b*-PVP),[1,2,9−11] polystyrene-*b*-poly(methyl methacrylate),[4,7,12,13] polystyrene-*b*-poly(ethylene oxide),[5,8,14,15] etc. The surface micelles exhibit various shapes from circular micelles to large planar aggregates via rod-shaped micelles mainly depending on the relative size of the two blocks. Circular micelles are formed at high hydrophilic block composition and prevail to as low as 15−20% content. As the composition of the hydrophilic block is reduced further, rod-shaped micelles are preferentially formed. If the hydrophilic block content is reduced as low as 5%, the uniform structure of surface micelles is no longer observed.

As the film is compressed, the area occupied by hydrophilic chains spread on the air−water interface is reduced, and it reaches a point at which the hydrophilic chains form a dense monolayer. Then the film goes through a transition at which the $\pi-A$ isotherm shows a plateau. The high compressibility of the film in the transition region has been understood as the hydrophilic corona chains dissolve into the subphase or make conformation transitions.[15]

In a sense, the surface micellization behavior is a two-dimensional analogue of the (three-dimensional) micellization of block copolymers in a selective solvent.[16] The structure of the three-dimensional aggregates formed by amphiphilic copolymers in selective solvents is determined by various factors such as relative block length,[17] ion contents,[18,19] solvent composition,[20] etc. The micelle formation of block copolymer containing ionizable block such as PVP has been a subject of interest in recent years.[21−27] The ionized PVP unit can carry counter metal cations that can be reduced to form various metal nanoparticles.[28] A number of studies on the pH dependence of the block copolymer micellization behavior have been also reported.[18,22,24,26,27] However, few studies were done for surface micelles with respect to the subphase pH change. The ionization of the hydrophilic block changes the solubility of the corona chain of the surface micelles and the electrostatic interaction between the ionized chains. In this work, we investigated the effect of subphase pH and ionic strength on the surface micellization behavior of PS-*b*-P2VP at the air−water interface.

Experimental Section

Samples. Polystyrene-*b*-poly(2-vinylpyridine) (PS-*b*-P2VP) diblock copolymers were synthesized by sequential anionic polymerization,

* Corresponding author: Tel +82-54-279-2109; Fax +82-54-279-3399; e-mail tc@postech.ac.kr.
† Department of Chemistry.
‡ Department of Materials Sciences and Engineering.

10.1021/ma052055x CCC: $33.50
Published on Web 12/15/2005

keeping the PS block length constant at 28 kg/mol and varying the P2VP block length at 11, 28, and 59 kg/mol (M_w/M_n = 1.08, 1.05, and 1.05, respectively) at −78 °C under an Ar atmosphere using *sec*-BuLi and THF as an initiator and a solvent, respectively. Details of the apparatus and the polymerization procedure were reported previously.[29,30] After the polymerization of styrene block was completed, an aliquot of the reaction mixture was withdrawn for characterization before 2VP monomer was added for the polymerization of the P2VP block. Subsequently, a series of diblock copolymers with an identical polystyrene block length were obtained by withdrawing aliquots of mixtures after each 2VP monomer addition. The average molecular weight and the molecular weight distribution of the PS blocks and the diblock copolymers were measured by gel permeation chromatography.

Langmuir−Blodgett (LB) Film. Langmuir films of the PS-*b*-P2VPs were formed at the air−water interface by spreading a dilute polymer solution in chloroform (0.5 mg/mL). The subphase was prepared with deionized water from a water purification system (Human, Seoul, Korea) equipped with an organic removal cartridge. The pH and ionic strength of the subphase were adjusted before the spreading of the polymer solution using phosphate buffers or strong acids such as hydrochloric acid or sulfuric acid. The surface pressure-surface area ($\pi-A$) isotherms were obtained using a Langmuir−Blodgett (LB) film apparatus (KSV 5000) at a compression rate of 5 mm/min. The temperature of the subphase was maintained at 25 °C using a circulating water bath (Neslab, RTE-110). LB films were transferred onto RCA-treated Si wafers at a constant vertical lift speed of 5 mm/min while keeping the surface pressure constant by compression. The transfer ratio of the LB film was close to unity. The LB films were examined by a tapping mode AFM (Digital Instruments, Nanoscope III). The AFM was housed in a vibration-resistant case, and silicon tips were used.

Results and Discussion

Figure 1 displays the $\pi-A$ isotherms of three different PS-*b*-P2VP block copolymers (28K−11K, 28K−28K, 28K−59K) at three different subphase pH in 0.2 M phosphate buffer. Although the situation at the air−water interface may be different from the bulk solution, if we assume that the ionization constant for pyridine in solution (pK_a = 5.2) is identical at the air−water interface, the pyridine residues in the P2VP block are fully ionized at pH 1.8. At pH 6.6, only a small fraction of the pyridine residues are ionized: the ratio of neutral to ionized pyridine is about 20. At pH 11.6, practically all the pyridine moieties are in the neutral form.

The difference in the $\pi-A$ isotherms at three pHs can be understood on the basis of the degree of ionization of the pyridine group. At pH 1.8, the surface pressure does not increase until the film was compressed to very low molecular area, indicating that not much surface-active material resides at the air−water interface regardless of the P2VP block length. The fully ionized P2VP blocks are no longer surface active and dissolved into the subphase almost completely. Therefore, a transition plateau representing the equilibrium between the floated and submerged corona chains is not observed. At higher pH, the $\pi-A$ isotherms are expanded, indicating that the partially ionized or neutral P2VP blocks are surface-active. At pH 6.6, the transition zone appears clearly for 28K−28K and 28K−59K samples at a surface pressure a little lower than 20 mN/m. The transition behavior is not observed for PS-*b*-P2VP with a shorter P2VP block (28K−11K). At pH 11.6 the $\pi-A$ isotherms are more expanded and the transition surface pressure increases further to a value higher than 20 mN/m.

The limiting areas of PS-*b*-P2VP were determined by extrapolating the linear region of π = 5−15 mN/m in the $\pi-A$ isotherms to the zero surface pressure and plotted in Figure 2. The limiting area is the virtual area occupied by a PS-*b*-P2VP molecule densely packed each other but uncompressed. The abscissa of Figure 2 is the molecular weight of the P2VP block represented as the number of 2VP monomers in the block. Then the slope of the plots is the area occupied by one 2VP monomer unit at the corresponding pH. The area occupied by a 2VP residue increases with pH, indicating that more 2VP monomers reside at the air−water interface (not submerged) at higher pH. At pH 1.8, the area is only 2.9 Å^2, confirming that most of the 2VP residues are submerged into the subphase.

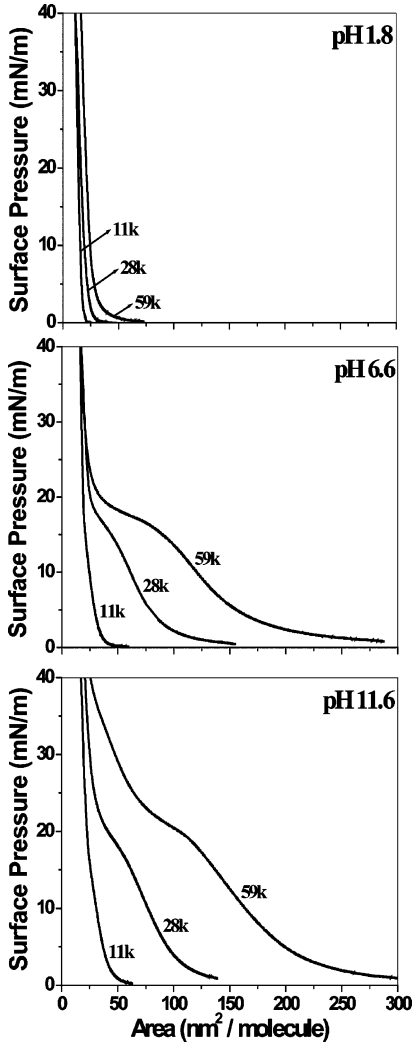

Figure 1. $\pi-A$ diagrams of PS-*b*-P2VP at three different subphase pH (0.2 M phosphate buffer). The molecular weights of the P2VP block are labeled for corresponding isotherms.

Except for the case of pH 1.8, the intercept of the plots approaches zero. This behavior was previously observed for many block copolymers forming surface micelles, which indicates that the PS block does not contribute significantly to the limiting area in this low surface pressure region.[5,11] It may indicate that the PS micelle cores lie on top of the P2VP monolayer in this surface pressure region. At pH 1.8, however, the plot shows a finite intercept, about 15 nm^2, which reflects a significant contribution of the PS surface micelle cores to the limiting area. Similar results are also obtained at higher pHs if the limiting area is determined at the surface pressure region above the transition pressure. Kumaki measured the area occupied by PS aggregates when a dilute solution of homo-PS was spread at the air−water interface.[31] The area was proportional to the molecular weight of PS, 4×10^{-4} MW = 11 nm^2 for 28 kg/mol, which is a little smaller than the limiting area of PS-*b*-P2VP at pH 1.8. The similar discrepancy was also

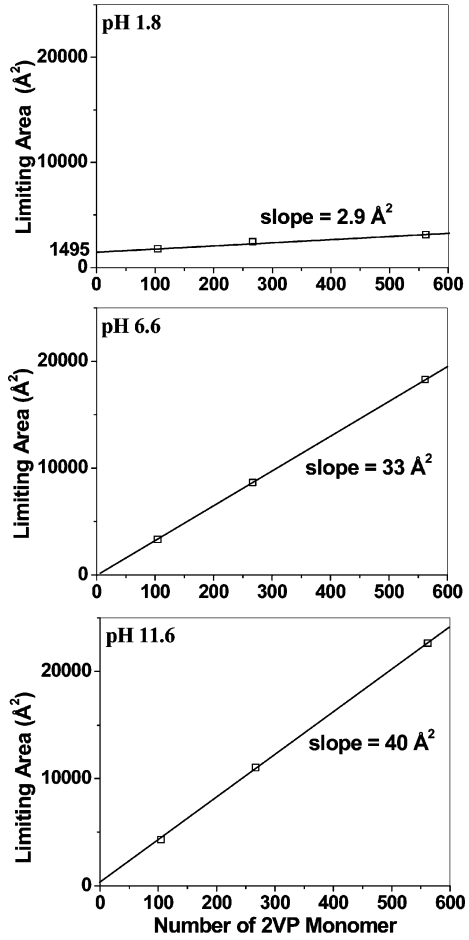

Figure 2. Limiting area per PS-*b*-P2VP molecule vs number of 2VP monomer in a molecule at three different pH, 1.8, 6.6, and 11.6, in 0.2 M phosphate buffer. The limiting areas were obtained by extrapolating the $\pi = 5-15$ mN/m region of the $\pi-A$ isotherms in Figure 1 to $\pi = 0$ mN/m.

observed for PS-*b*-PEO and ascribed to the contribution of submerged chains to the limiting area.[5]

Figure 3 shows the AFM topographic images of the three PS-*b*-P2VP LB films prepared at the subphase pH 1.8 and 6.6 in 0.2 M phosphate buffer. The LB films were transferred at a surface pressure of 2 mN/m that is far below the transition surface pressure. For 28K−11K sample, circular micelles coexist with rod-shaped micelles due to the relatively short P2VP block length. Also, there is no clear difference in morphology at the two different pHs. In contrast, for 28K−28K and 28K−59K samples, a big morphological difference shows up between the LB films deposited at the two different pHs. At pH 6.6, isolated circular micelles are observed for both block copolymers, which is the morphology commonly observed for amphiphilic block copolymers with large hydrophilic blocks. The distance between the PS cores reflects the hydrophilic P2VP block length residing at the air−water interface as corona chains. At pH 1.8, however, the circular micelles are in contact with each other to form a laced network structure, but certainly not rod-shaped micelles. The reduction of the intermicellar distance is an expected phenomenon since the area pervaded by the P2VP corona at the air−water interface decreases due to the increased solubility of P2VP at low pH. However, it is intriguing that they neither remain as isolated circular micelles nor make randomly associated structure, but are connected to form the laced array of circular micelles. This laced array is contradictory to a simple-minded expectation that the circular micelles would repel each other due to the highly ionized P2VP blocks. To our knowledge, this is a new morphology found for two-dimensional surface micelles.

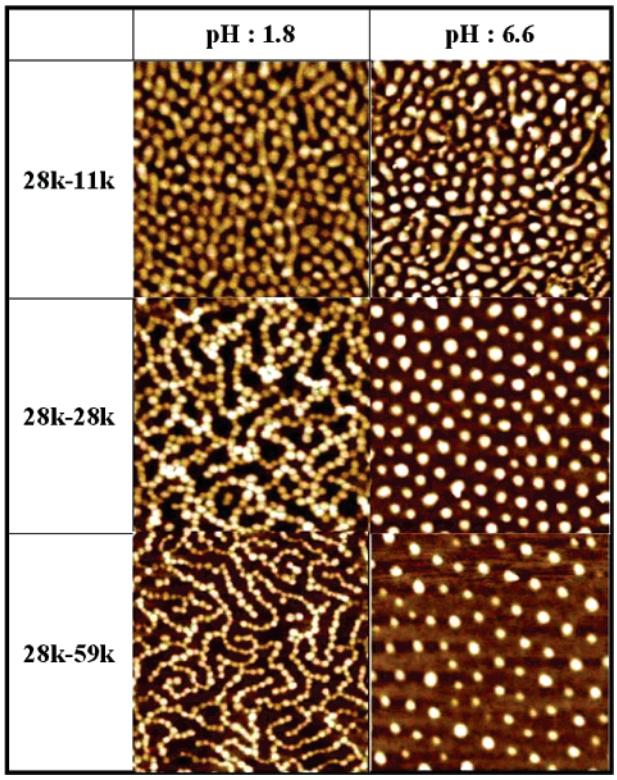

Figure 3. AFM images (1×1 μm) of PS-*b*-P2VP Langmuir−Blodgett films deposited at $\pi = 2$ mN/m (subphase: 0.2 M phosphate buffer).

To examine the laced surface micelle structure at low pH in more detail, the LB films of the 28K−59K sample were prepared at different surface pressures at pH 1.8 in 0.2 M phosphate buffer, and the morphology of the LB film was measured by AFM. As displayed in Figure 4a, without any compression of the Langmuir monolayer after spreading of PS-*b*-P2VP ($\pi = 0$ mN/m), the circular micelles already start to associate. The extent of association is not large at $\pi = 0$ mN/m, but all the associated micelles have linearly laced structure. The length of the laced array increases as the film is compressed, and a few branches show up at $\pi = 2$ mN/m (Figure 4b). As the film is compressed further, the circular micelles make more random connections. These observations indicate that the association of the PS micelle cores with ionized P2VP brush is a spontaneous process, which is likely to be driven by the hydrophobic interaction between the PS micelle cores. We will come back to this later.

To examine the pH-dependent surface micellization behavior of PS-*b*-P2VP more quantitatively, the average aggregation number in a surface micelle was calculated at different subphase pH at 2 mN/m, and the results are summarized in Table 1. The results at pH 5.3 (pure water) are included from the previous report.[11] The average aggregation number per surface micelle was determined by dividing the number of PS-*b*-P2VP molecules in a fixed surface area (1×1 μm) with the number of circular micelles in the same area counted from the AFM image. The aggregation number is larger for the 28K−28K sample than 28K−59K, which is in accord with the known trend found in various block copolymer surface micelles; the aggregation number in a surface micelle decreases as the ratio of the hydrophobic block size to hydrophilic block size decreases.[3,7,8] In this regard, it is expected that the aggregation number is also

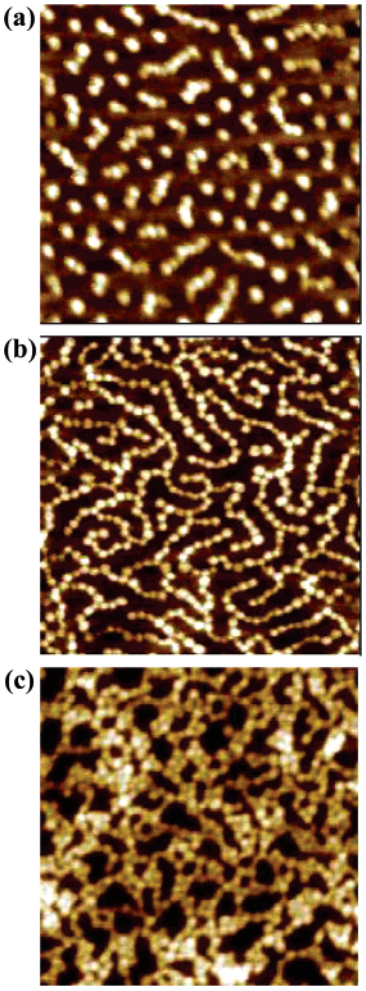

Figure 4. AFM images (1 × 1 μm) of 28K−59K PS-*b*-P2VP Langmuir−Blodgett films deposited at three different surface pressures: 0 (a), 2 (b), and 10 mN/m (c) at pH 1.8 in 0.2 M phosphate buffer.

Table 1. Number Density[a] and Average Aggregation Numbers of Surface Micelles at Different pHs[b]

	no. of micelles/μm^2	aggregation no.
	(a) 28K−28K Sample	
pH 1.8	486 ± 18	71 ± 3
pH 5.3 (pure water)	143 ± 2	74 ± 1
pH 6.6	125 ± 6	78 ± 5
pH 11.6	121 ± 11	70 ± 6
	(b) 28K−59K Sample	
pH 1.8	614 ± 10	47 ± 1
pH 4.1	79 ± 3	51 ± 2
pH 5.3 (pure water)	103 ± 2	51 ± 1
pH 6.6	91 ± 5	51 ± 3
pH 11.6	86 ± 8	47 ± 5

[a] Average number of surface micelles in 1 × 1 μm area from the AFM image. [b] Uncertainty is one standard deviation obtained from the analysis of four separate 1 × 1 μm AFM images of the LB films transferred at π = 2 mN/m.

affected by the degree of ionization. As shown in Table 1, however, the aggregation number is independent of pH within the experimental precision.

Another interesting feature found from the results in Table 1 is in the micelle number density. In general, the number density of surface micelles decreases with pH increase since less ionized P2VP chains should have a tendency to float at the surface and pervade a larger area than the highly ionized chains. However, the number density of surface micelles of the 28K−59K sample

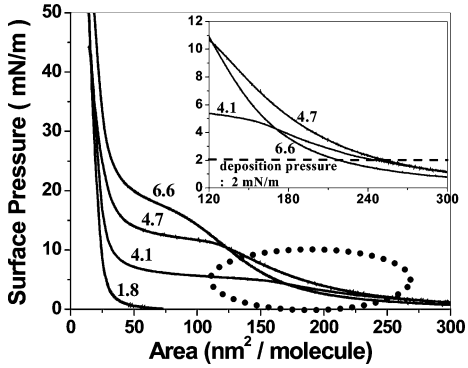

Figure 5. π−*A* isotherms of the 28K−59K sample obtained at different subphase pHs in 0.2 M phosphate buffer. Each π−*A* isotherms is labeled with the corresponding subphase pH. In the inset, an expanded portion of the isotherms is displayed.

is exceptionally low at pH 4.1. The complex behavior was investigated further by π−*A* isotherm measurements. Figure 5 shows π−*A* isotherms of the 28K−59K sample at four different pHs in 0.2 M phosphate buffer. The π−*A* isotherms measured at pH 4.1 and 4.7 exhibit highly stretched transition regions (very high compressibility). As a result, at low surface pressure they cross the π−*A* isotherm at pH 6.6 and the PS-*b*-P2VP has a larger molecular area at pH 4.1 and 4.7 than at pH 6.6. It is consistent with the fact that the number density of micelles at pH 4.1 is peculiarly small in Table 1.

Despite the consistency among the experimental results, it is not straightforward to understand how the more highly ionized P2VP block at pH 4.1 or 4.7 can occupy a larger molecular area than pH 6.6. These interesting phenomena found in PS-*b*-P2VP surface micelles could be understood in terms of the balance among the solubility of the ionized P2VP chains, the electrostatic repulsion between the ionized pyridine moieties, and the hydrophobic interaction between the PS micelle cores. At around pH 4.1, the effects of the solubility and electrostatic repulsion of P2VP chains would be balanced in such a way that the Langmuir film exhibits the stretched transition region with a high compressibility at low surface pressure. In other words, at pH 4.1 the partially ionized P2VP chains do not spontaneously submerge into the subphase but reside at the air−water interface at low surface pressure. At the same time, the electrostatic repulsion stretches the P2VP chains to occupy a large area pervaded by each P2VP chain. Upon compression of the Langmuir film, the partially ionized P2VP chains occupying the large area submerge into the subphase extending the transition plateau. Since the ionized P2VP chains easily submerge into the subphase, the Langmuir film shows very high compressibility at low surface pressure.

As pH is further lowered (pH = 1.8), the solubility of the fully ionized P2VP chain becomes high enough to submerge into the subphase even in the absence of the compression force. They are no longer able to reside at the air−water interface, and little surface pressure is observed until the PS micelle cores with submerged P2VP chains feel repulsive interaction each other as the Langmuir film is compressed. The PS micelle cores floating at the air−water interface do not have sufficient P2VP chain corona to protect their hydrophobic surface and associates each other driven by the hydrophobic interaction. Such an association of hydrophobic particles was observed earlier for PS monomolecular particles formed at the air−water interface by spreading dilute PS solution.[31] While the PS particles associate randomly, the PS-*b*-P2VP surface micelles with ionized P2VP brush form a laced structure with little branches. It is seemingly due to the electrostatic repulsion between the

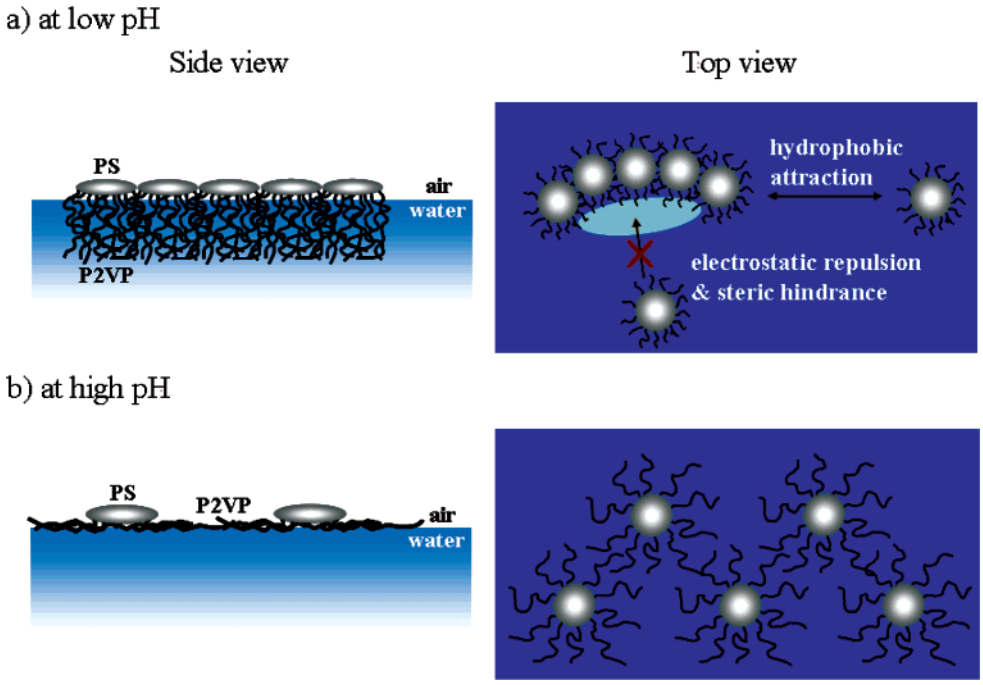

Figure 6. Schematic illustrations of the formation of laced micelles at low pH (a) and isolated circular micelles at high pH (b).

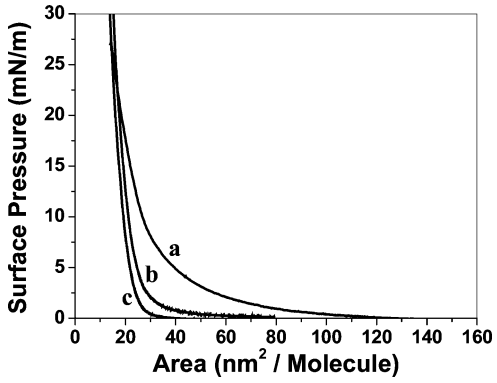

Figure 7. $\pi-A$ isotherms of PS-*b*-P2VP (28K−28K) at pH 1.8, but at three different ionic strengths: (a) 6.0×10^{-3}, (b) 2.8×10^{-2}, and (c) 0.12 M.

highly charged P2VP chains submerged in the subphase. Figure 6 schematically illustrates the formation of laced micelles at low pH (a) and isolated surface micelles at high pH (b).

To verify the picture outlined above, we investigated on the effect of the subphase ionic strength. Figure 7 displays the $\pi-A$ isotherms of 28K−28K sample at pH 1.8 but at different ionic strengths: (a) 6.0×10^{-3} M hydrochloric acid, (b) 6.0×10^{-3} M sulfuric acid, and (c) 0.2 M phosphate buffer. Since the pH of the former two cases were adjusted by adding NaOH solution, the ionic strength of the three different subphases are (a) 6.0×10^{-3} M, (b) 2.8×10^{-2} M, and (c) 0.12 M. The $\pi-A$ isotherms show the ionic strength effect at the same subphase pH. As the ionic strength of the subphase increases, the isotherms show the more condensed film behavior. It is clear that the electrostatic repulsion among the charged P2VP chains is screened more effectively at higher ionic strength media so that the Langmuir film of the surface micelles can be compressed without surface pressure increase until more hard-core-like repulsion among the surface micelles increases the surface pressure abruptly.

The ionic strength effect is also evident from the AFM images shown in Figure 8, which display the topography of LB films of the 28K−28K sample transferred at $\pi = 2$ mN/m from the subphase corresponding to Figure 7a,b. Even at pH = 1.8, most

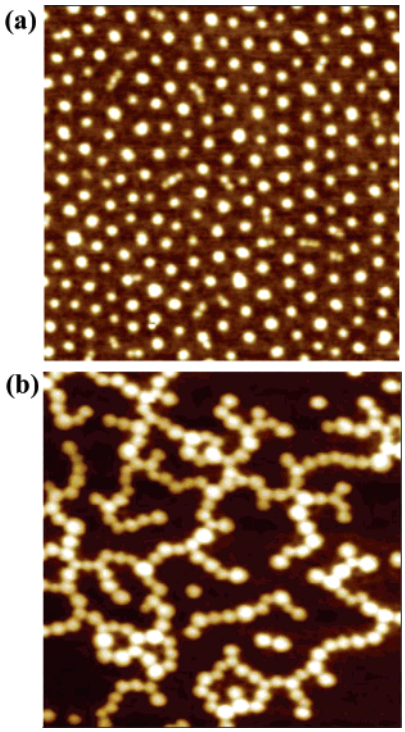

Figure 8. AFM images ($1 \times 1\ \mu$m) of LB films of PS-*b*-P2VP (28K−28K) transferred from the subphase $\pi = 2$ mN/m at pH 1.8 but at different ionic strengths: (a) 6.0×10^{-3} and (b) 2.8×10^{-2} M.

of the surface micelles exist as separated circular micelles at the low ionic strength while they associate to form the laced structure at high ionic strength. The $\pi-A$ isotherms and the AFM images of the LB film shown in Figures 7 and 8 support the proposition that the laced structure of PS-*b*-P2VP surface micelles results from the balance of the hydrophobic interaction between the PS micelle cores and the electrostatic repulsion between the ionized P2VP blocks. Also, it is worthwhile to note that the association of diblock copolymer micelles has been found in aqueous solution upon increasing the ionic strength.[32]

In summary, we investigated the surface micelle behavior of PS-*b*-P2VP at various subphase pH by $\pi-A$ isotherm and the surface morphology of the LB film. The block copolymers were prepared by anionic polymerization to have a constant PS block length at 28 kg/mol and varying P2VP block length of 11, 28, and 59 kg/mol. At high pH, PS-*b*-P2VP showed the $\pi-A$ isotherms characteristic of the block composition with partially ionized or un-ionized P2VP corona chains residing at the air−water interface. On the other hand, at low pH, fully ionized P2VP blocks are no longer surface-active and dissolved into the subphase. As a result, the $\pi-A$ isotherms of PS-*b*-P2VP at different composition become similar at low pH. Furthermore, the circular micelles associates to form a laced network structure at low pH. The dependence of the micelles association on surface pressure and the subphase ionic strength indicates that the formation of necklace structure can be understood as a balance of the hydrophobic attraction between the PS cores and the electrostatic repulsion between the ionized P2VP blocks submerged in the water.

Acknowledgment. This study was supported by a grant from Korea Research Foundation (KRF-2004-005-D00005) and the BK21 program.

References and Notes

(1) Zhu, J.; Eisenberg, A.; Lennox, R. B. *J. Am. Chem. Soc.* **1991**, *113*, 5583.
(2) Zhu, J.; Lennox, R. B.; Eisenberg, A. *J. Phys. Chem.* **1992**, *96*, 4727.
(3) Zhu, J.; Eisenberg, A.; Lennox, R. B. *Macromolecules* **1992**, *25*, 6547.
(4) Lin, B.; Rice, S. A. *J. Chem. Phys.* **1993**, *98*, 6561.
(5) Goncalves da Silva, A. M.; Filipe, E. J. M.; d'Oliveira, J. M. R.; Martinho, J. M. G. *Langmuir* **1996**, *12*, 6547.
(6) Baekmark, T. R.; Sprenger, I.; Ruile, M.; Nuyken, O.; Merkel, R. *Langmuir* **1998**, *14*, 4222.
(7) Seo, Y.; Paeng, K.; Park, S. *Macromolecules* **2001**, *34*, 8735.
(8) Baker, S. M.; Leach, K. A.; Devereaux, C. E.; Gragson, D. E. *Macromolecules* **2000**, *33*, 5432.
(9) Zhu, J.; Lennox, R. B.; Eisenberg, A. *Langmuir* **1991**, *7*, 1579.
(10) Goren, M.; Lennox, R. B. *Nano Lett.* **2001**, *1*, 735.
(11) Choi, M.; Chung, B.; Chun, B.; Chang, T. *Macromol. Res.* **2004**, *12*, 127.
(12) Seo, Y.; Im, J.; Lee, J.; Kim, J. *Macromolecules* **2001**, *34*, 4842.
(13) Chung, B.; Park, S.; Chang, T. *Macromolecules* **2005**, *38*, 6122.
(14) Goncalves da Silva, A. M.; Gamboa, A. L. S.; Martinho, J. M. G. *Langmuir* **1998**, *14*, 5327.
(15) Cox, J. K.; Yu, K.; Constantine, B.; Eisenberg, A.; Lennox, R. B. *Langmuir* **1999**, *15*, 7714.
(16) Förster, S.; Abetz, V.; Müller, A. H. E. *Adv. Polym. Sci.* **2004**, *166*, 173.
(17) Zhang, L. F.; Eisenberg, A. *Science* **1995**, *268*, 1728.
(18) Zhang, L. F.; Yu, K.; Eisenberg, A. *Science* **1996**, *272*, 1777.
(19) Ito, H.; Imae, T.; Nakamura, T.; Sugiura, M.; Oshibe, Y. *J. Colloid Interface Sci.* **2004**, *276*, 290.
(20) Yu, G.; Eisenberg, A. *Macromolecules* **1998**, *31*, 5546.
(21) Antonietti, M.; Heinz, S.; Schmidt, M.; Rosenauer, C. *Macromolecules* **1994**, *27*, 3276.
(22) Martin, T. J.; Prochazka, K.; Munk, P.; Webber, S. E. *Macromolecules* **1996**, *29*, 6071.
(23) Esselink, F. J.; Dormidontova, E. E.; Hadziioannou, G. *Macromolecules* **1998**, *31*, 4873.
(24) Shen, H.; Zhang, L.; Eisenberg, A. *J. Am. Chem. Soc.* **1999**, *121*, 1, 2728.
(25) Tsitsilianis, C.; Voulgaris, D.; Stepanek, M.; Podhajecka, K.; Prochazka, K.; Tuzar, Z.; Brown, W. *Langmuir* **2000**, *16*, 6868.
(26) Gohy, J.-F.; Willet, N.; Varshney, S.; Zhang, J.-X.; Jerome, R. *Angew. Chem., Int. Ed.* **2001**, *40*, 3214.
(27) Gohy, J.-F.; Antoun, S.; Jerome, R. *Macromolecules* **2001**, *34*, 7435.
(28) Förster, S.; Antonietti, M. *Adv. Mater.* **1998**, *10*, 195.
(29) Kwon, K.; Lee, W.; Cho, D.; Chang, T. *Korea Polym. J.* **1999**, *7*, 321.
(30) Lee, W.; Cho, D.; Chang, T.; Hanley, K. J.; Lodge, T. P. *Macromolecules* **2001**, *34*, 2353.
(31) Kumaki, J. *Macromolecules* **1988**, *21*, 749.
(32) Förster, S.; Hermsdorf, N.; Leube, W.; Schnablegger, H.; Regenbrecht, M.; Akari, S.; Lindner, P.; Bottcher, C. *J. Phys. Chem. B* **1999**, *103*, 6657.

MA052055X